The Role of divalent transition Metal ions in the binding of Fur dimer to DNA: Binding of Mn^{2+} and Co^{2+} to EC Fur dimer-DNA complex

Mazen Y. Hamed*
Chemistry Department, Birzeit University, PoBox 14, Birzeit, Palestine
Salih Jabour+
Faculty of Medicine and Medical studies, Jerusalem University, Palestine

* Corresponding author: mhamed@birzeit.edu

Abstract

Ferric uptake regulation protein is a repressor protein which binds an AT rich region of DNA (the iron box). Fur binds as a dimer in a helix turn helix mode and it is activated by iron(II) and other transition metal ions at elevated concentrations. Each transition metal ion induces certain conformational changes to aid the Fur binding, both the N-terminal domain (Ala11 to Pro18) and residues in the αHelices near the C-terminal domain (Asp137 to His135) take part in binding to DNA in addition to residues in the area His 90 to His 86. The process is discussed in view of experimental reports. Fe(II), Mn(II) and Co(II) activate Fur to bind DNA but Zinc plays a structural role and does not activate Fur to bind DNA.

Graphical Abstract:
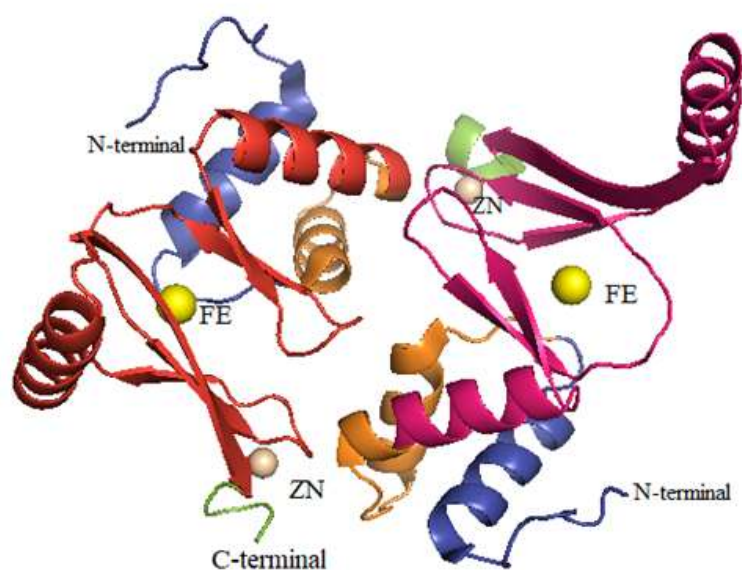
Keywords: Ferric Uptake Regulation; Fur, Iron(II), Molecular dynamics; DNA; protein.

Introduction

Fur protein regulates the iron uptake in living cells by binding a 19-bp TATA called the iron or Fur box[1][2]. In previous work [3] [4] [5] [6], we have established that Fur dimer binds DNA in the presence of divalent metal ions as co-repressors [3], Fur protein employs the helix turn helix (HTH) mode in its DNA binding and using Fe^{2+} as co-repressor in the biological systems to bind the DNA as a dimer [2]. Experimentally, Fe^{2+}, Co^{2+} [7] and Mn^{2+} acted as co-repressors to activate Fur binding to the DNA[2] while Zn^{2+}, Fe^{3+}, Cd^{2+} failed to activate Fur binding[2][8]. Zn^{2+} ion plays a structural role [9][10] [11], Fur dimer isolated from cells was reported to contain a structural zinc ion[12], recently the crystal structure of Mur tetramer with 8 zinc ions (2ions/Fur)[13]. The crystal structure of a Fur dimer with $11Mn^{2+}$ ions and $12 Zn^{2+}$ ions was reported [14]. indeed, we reported a first zinc ion site in which zinc ion is bound to C92, C95, H140 and Asp 137[9,15] and this is recognized as the zinc site, there are no reported crystal structures with Fur bound to DNA. This work is aimed to give more insight on the crucial role of different transition metal ions (as co-repressors) and the ability of HTH in DNA binding proteins to accommodate more than one type of transition metal ion in their designed pockets (metal ion sites), at the same time, to make these ions capable of activating the repressor protein to bind specific DNA target.

Is there an effect for varying the divalent transition metal ion on the process of Fur binding to DNA and the role each metal ion plays in the conformational changes that take place in both Fur dimer and DNA in order

to enhance the DNA binding process? An important aspect which will be discussed further in this study to help in understanding the vital role for metal ions in this process, does the metal ion play a structural role only, or does it have other functions to perform to make the specific binding successful.

Fur, being a global repressor activator protein capable of binding many genes. This gave the Fur repressor the flexibility to be activated by more than one transition metal ion in addition to its naturally occurring co-repressor Fe(II). Fur binds Mn (II), Zn(II), Cu(II), Cd(II) and Co(II) and is activated by these ions to various degrees and it has varying affinities towards each ion. Previous studies[4] [2][8][16] [17] [18] showed that all these ions bind the same pockets on the Fur dimer. Experimental dissociation constants using equilibrium studies showed that Fur dimer binds metal ions in nM quantities to be activated to bind DNA[8]. Molecular dynamics studies yield a great deal of information which can be helpful in supporting the experimental findings on the fine tuning process of Fur protein by metal ions to bind specific DNA bases in a HTH mode, and to better understand the structure-function relationship of this class of DNA binding repressor proteins and there specificity to certain genes[3].

The study was extended to Mn (II), Co (II) binding in order to shed more light on this binding process and to obtain more information on the metal ion sensing process and the structural role metal ions play in the process as a whole.

Mn(II) is always used experimentally to replace the naturally occurring co-repressor ion Fe(II), both in vivo and in vitro due to its stability over Fe(II) and ease of handling because Fe(II) easily oxidizes, in addition to

the role Mn(II) plays in biological processes which involves Fur binding to DNA.

The secrets of metal ion role in protein binding to DNA are revealed in this paper which will aid in better understanding of the role of metal ions in the DNA binding process [19], it becomes more established that metal ions play a structural role in addition to aiding the tuning mechanism of the protein dimer to a perfect, but not lasting fit on the DNA sequence. It is worth mentioning that none of the Fur crystal structures reported shows its DNA binding.

Computational Methods

All the molecular dynamics simulations(MD) were performed using AMBER molecular simulation package [20] . AMBER force field was used for molecular minimization and molecular dynamics. The analyses of MD trajectories were also preformed using AMBER. *Pymol* molecular viewer package was used for visualization [21].

Homology modeling of Fur protein

The known Fur sequence (from E. coli) was submitted to different modeler servers in order to predict the three- dimensional structure. SWISS MODEL [22], PHD, 3DPSSM[23] and VADAR servers were used to align the Fur sequence with similar known proteins Data Bank and compared to the reported crystal structures without the presence of DNA[13] [24] [10]. Several templates for Fur protein were generated while the sequence with high similarity served as a reference sequence. The superposition of each atom was optimized by maximizing Ca in the common core while minimizing their relative mean square value deviation (RMSD) at the same time. Spare part algorithm was used to search for fragments that can be accommodated into the framework of the Brookhaven Protein Data Bank

(PDB). The coordinates of central backbone atoms (N, O and C) were averaged, and then added to the target model. The side chains were added according to the sequence identity between the model and the template sequence. AMBER was used to idealize the geometry for bonds and also to remove any unfavorable non-bonded contacts. This was done by minimizing the energy. All hydrogen atoms were added and the apo-Fur structure was subjected to a refinement protocol with constraints on the Fur structure gradually removed. 100 steps of steepest descent, followed by 300 steps of conjugate gradient algorithm were applied during energy minimization. The energy minimization process on the apo-Fur model was performed, first in vacuum and in H_2O as solvent using TIP3P in Amber with 12 Å box , nine Na^+ ions were added to the model to neutralize the system.

Building the Fur dimer AUTODOCK [25] was used to generate the apo-Fur dimer. Two molecules of the previously determined structure for the apo-Fur monomer were docked on each other, and the best docking sites were predicted. Monte Carlo (MC) simulated annealing (SA) algorithm was used for exploring the Fur configuration by a rapid energy evaluation technique using a grid-based molecular affinity potential. The energy of interaction, affinity and the grid for electrostatic potential were evaluated using the Poisson–Boltzmann finite difference method and were assigned to each atom.

Docking of the apo-Fur dimer onto a 19 bp fragment representing the DNA: Nucgen suite program (part of the AMBER package was used to build the Cartesian coordinates for canonical B- model of the iron box (a 19-bp inverted repeat sequence designated the iron box (5' – GATAATGATAATCATTATC - 3'); the proposed recognition site of Fur on the DNA. The right-handed B-DNA duplex conformation was applied for

the model. The iron box was docked to the Fur-dimer using the AUTODOCK program. The energy minimization was applied to the resultant model in order to refine the Fur dimer –DNA complex. The parameters file for the iron metal was built manually and inserted into AMBER as a library file. The first scenario was using 4 Fe^{2+} ions per Fur dimer–DNA complex in the water environment and adding Na+. MD simulations were carried out at 300 K. Explicit solvent model TIP3P water was used as solvent model. The models were solvated with a 12 A˚ water cap from the center of mass of the ligands. The dynamics simulation was applied for 200 ns time limit. In a second scenario, the same was repeated using 8 Fe^{2+} ions and simulation was applied for 200 ns.

Results and Discussion

Proteolytic enzymes were used to detect metal-induced conformational changes in the ferric uptake regulation (Fur) protein of Escherichia coli. Metal binding results in DNA binding which showed similar metal ion specificity and concentration dependencies, suggesting that the conformational change detected is required for operator DNA binding[17]. Isolation and characterization of biochemically generated fragments of Fur as well as other data indicate that the N-terminal region is necessary for the interaction of the repressor with DNA and that a C-terminal domain is sufficient for binding to metal ions [26].

The interaction of the Ferric Uptake Regulation (Fur) protein with the backbone of operator DNA was analyzed by hydroxyl radical foot printing [17]. Contacts made by Fur and those made by the helix-turn-helix proteins shows that the mode of DNA binding by this repressor is unique. Experiments demonstrate that Fur-operator contacts are segregated on one face of the helix and span nearly three successive major grooves. Indeed, our

molecular dynamics simulation shows that all studied metal ions were found to induce parallel changes in the Fur dimer conformation as can be seen in (Figures1 and 2), the shifts in residue positions towards DNA changes upon varying the metal ion type, concentration and using a mix of two different ions.
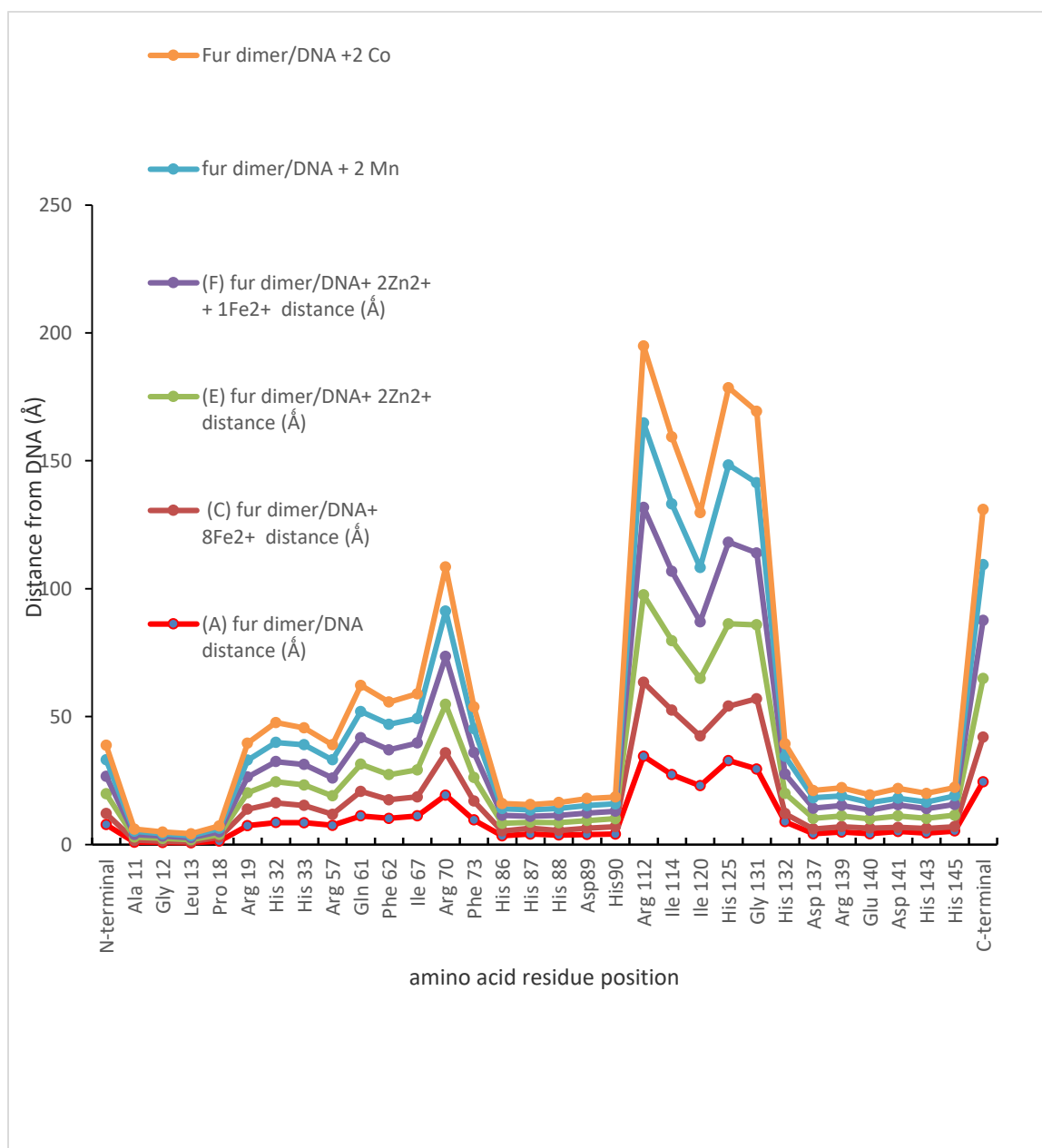
Figure 1 (a): Conformational changes of the Fur EC dimer and DNA binding. Calculated distances between the amino acid residues of Fur and

the AT-unit in the B-canonical DNA. Fur dimer and DNA fragment with no metal ion present (red). Fur dimer and DNA in the presence of Fe^{2+} ions (brick red). Fur dimer and DNA in presence of two Zn^{2+} ions (Green). Fur dimer and DNA in presence of two Zn^{2+} and one Fe^{2+} ions (purple). Fur dimer and DNA in presence of two Mn^{2+} ions (light blue). Fur dimer and DNA in presence of two Co^{2+} ions (Orange).
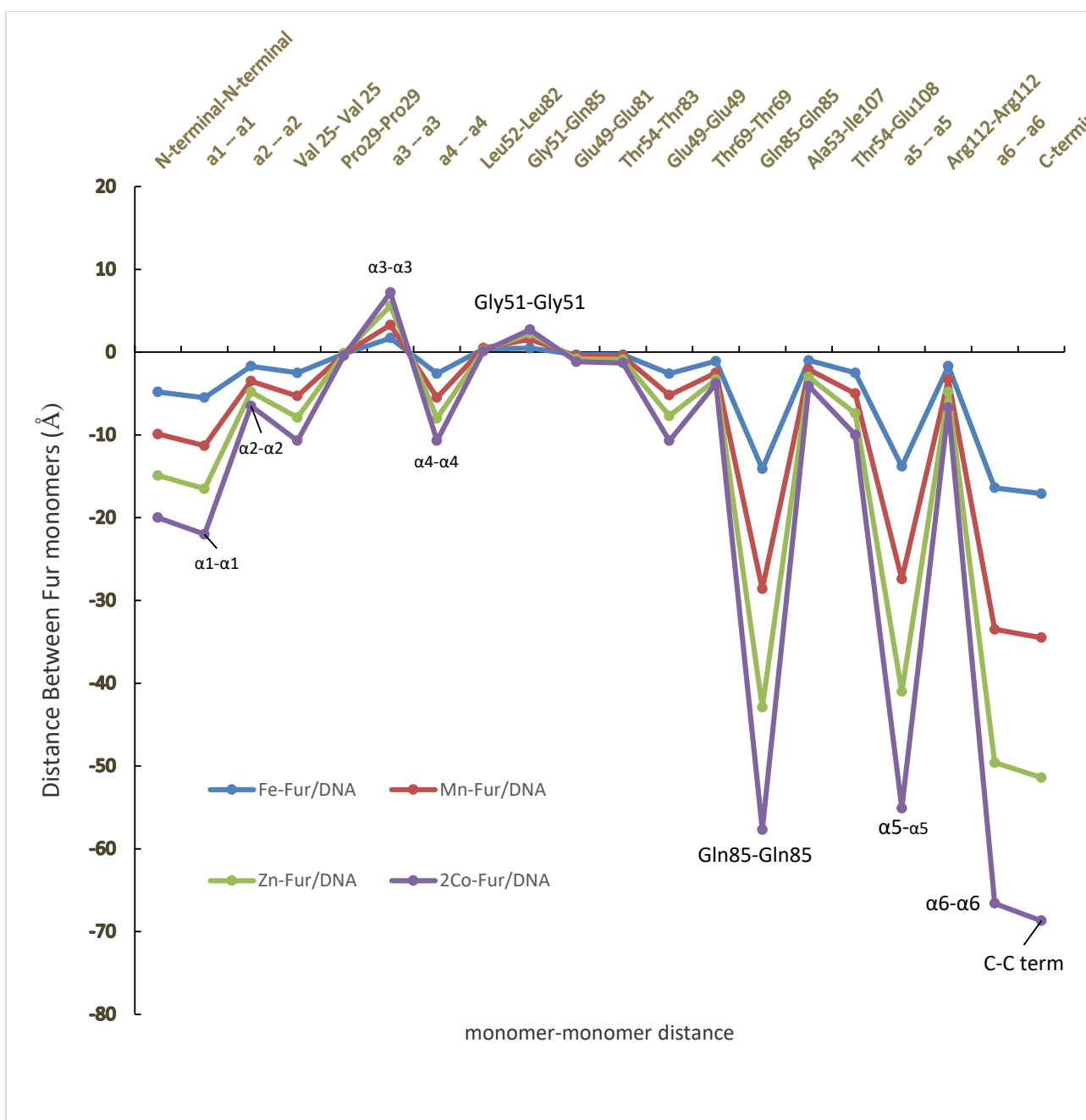
Figure1(b): The Fur monomer-monomer distance in the presence of DNA iron box represented by key positions: Conformational changes of the Fur EC dimer induced by DNA and Fe^{2+} binding. Measured Distances between residues and helices on one Fur subunit and the other. All values measured relative to apo-Fur dimer/DNA. Apo-Fur/DNA +Fe^{2+} (blue circles and blue

line); Fur/DNA in the presence of Zn^{2+} ions (green); Fur/DNA in presence of Mn^{2+} ions (brick red); Fur/DNA in the presence of Co^{2+} ions (purple).

This plot Figure 1(a) shows that there are three major contact regions on the Fur protein to the DNA: The first consists of residues Ala11, Gly12, Leu13 Pro18 and Arg19 near the N-terminal, the second is His88 to Arg112, and the third region consists of residues139–145 near the C-terminal and this region is the closest to the DNA. These findings are in agreement with experimental work[17][26].
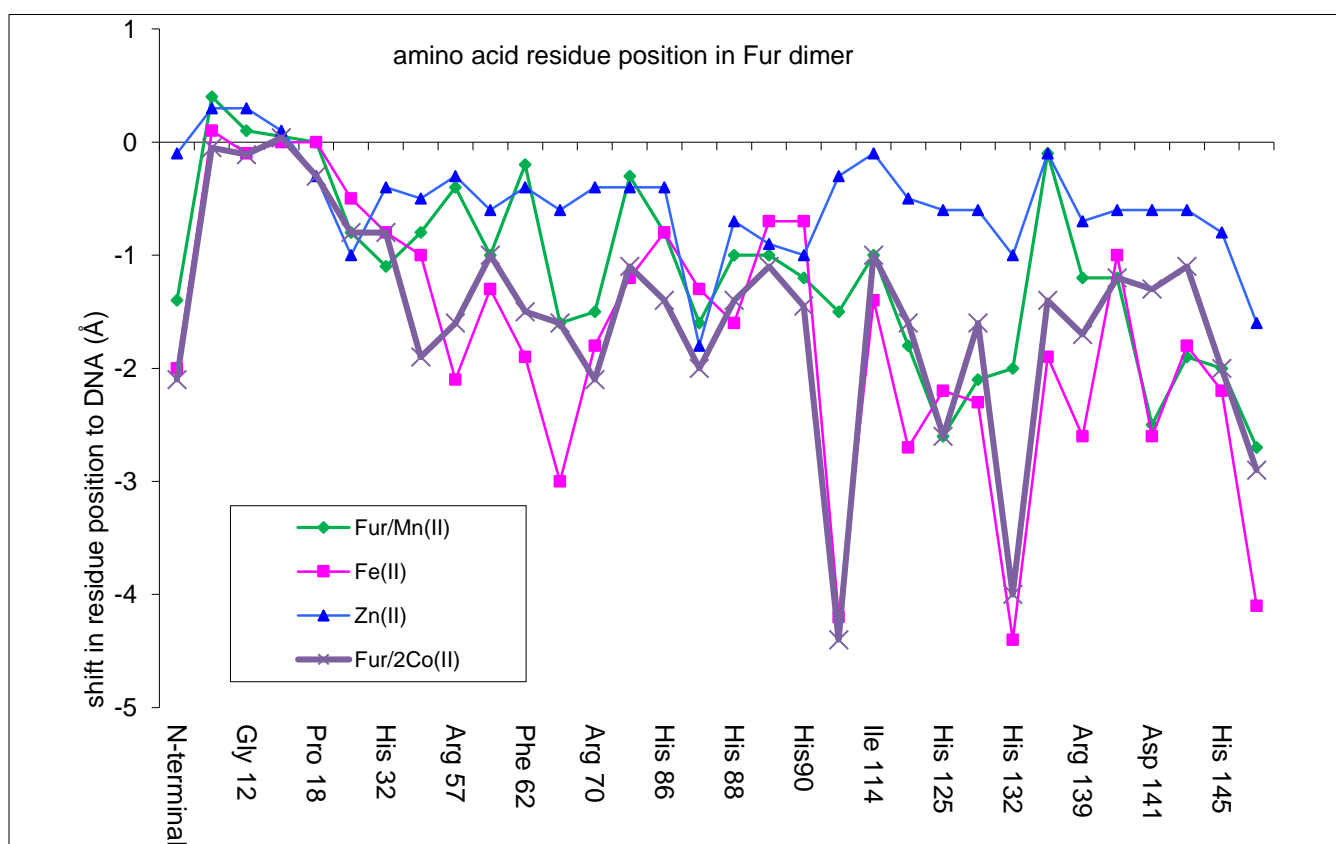
Figure 1(C): Effect of adding metal ions on shifting the Fur dimer residues closer to DNA. Plots were taken as difference between the position of apo-Fur dimer with no metal ion present and those of Fur/DNA with metal ion present [(M^{2+}/Fur/DNA)–Apo-Fur/DNA)]: The change in Fur-DNA

Table1: The calculated Metal ion residue distances on Fur showing the effect on M^{2+} --Ligand distance upon changing the metal ion and increasing the metal ion ratio from 1:1 to 2M:1 Fur

Residue	M^{2+}Fur (Å)[1]	Fur dimer/ DNA + M^{2+}	Fur dimer/ DNA + $2Zn^{2+}$	Fur dimer/DNA + $2Zn^{+2}$ +1 Fe^{2+}	Fur dimer/DNA + $2Zn^{2+}$ + $2Fe^{2+}$	fur dimer/DNA + 2 Mn	$1co^{2+}$	2 co^{2+}
Site 2								
M-His 71	Fe^{2+}(1.3)		Zn^{2+} 2.1	Zn^{2+} 3.4	Fe^{2+} 2.6	2		1.8
M-Ile 50	Fe^{2+}(2.3)		Zn^{2+} 2.5	Zn^{2+} 5.8	Fe^{2+} 2.1	2.1		2.1
M-Asn 72	Fe^{2+}(1.5)		Zn^{2+} 2.1	Zn^{2+} 6.5	Fe^{2+} 3.1	2.5		1.7
M-Gly 97	Fe^{2+}(2.3)		Zn^{2+} 3.1	Zn^{2+} 7.7	Fe^{2+}2.4	2.5		2.4
M-Asp 105	Fe^{2+}(1.4)		Zn^{2+} 2.3	Zn^{2+} 6.2	Fe^{2+} 2.7	2.8		1.9
M-Ala 109	Fe^{2+}(2.1)		Zn^{2+} 2.8	Zn^{2+} 5.9	Fe^{2+} 1.9	2.2		2.2
Site 1 (Zn site)								
M-Cys 92	Fe^{2+}(2.2)	Zn^{2+} (3.2)	Zn^{2+} 2.9	Fe^{2+} 2.5	Fe^{2+} 2.2	2.3	2.8	2.1
M-Cys 95	Fe^{2+}(1.6)	Zn^{2+} (2.9)	Zn^{2+} 2.7	Fe^{2+} 2.6	Fe^{2+} 2.3	1.8	2.6	2
M-Asp 137	Fe^{2+}(1.3)	Zn^{2+} (3.1)	Zn^{2+} 3.1	Fe^{2+} 2.5	Fe^{2+}2.7	2.9	3	2.2
M-Asp 141	Fe^{2+}(1.5)	Zn^{2+} (3.2)	Zn^{2+} 3.0	Fe^{2+} 2.9	Fe^{2+}3.1	3.2	2.7	1.8
M-Arg 139	Fe^{2+}(1.7)	Zn^{2+} (4.1)	Zn^{2+} 3.6	Fe^{2+} 3.0	Fe^{2+}2.8	2.7	3.1	2.2
M-Glu 140	Fe^{2+}(1.3)	Zn^{2+} (2.1)	Zn^{2+} 1.8	Fe^{2+} 1.2	Fe^{2+}1.7	1.5	1.4	1.2
M –His 145	Fe^{2+}(1.2)	Zn^{2+} (2.4)	Zn^{2+} 2.1	Fe^{2+} 2.0	Fe^{2+}1.9	2.1	1.5	1.3
M-His 143	Fe^{2+}(1.5)	Zn^{2+} (2.5)	Zn^{2+} 2.5	Fe^{2+} 2.3	Fe^{2+}2.1	2.4	1.7	1.4

distances represented by key amino acid residues upon adding metal ions:
(1) Zn^{2+} (Blue triangles and blue line. (2) After adding Mn^{2+} green (3) After
adding Fe^{2+} pink, (4) after adding two Co^{2+}per Fur (purple).

Figure 1(C)   gave insight on the primary role of metal ion in shifting
the residue positions closer to DNA bases in addition to inducing different
conformations in the helices of Fur protein Figure 1(b).

This is, possibly, more important role for metal activation of Fur, although
the structural role and effect on confirmation are inseparable. The sensitivity
of binding to metal ion concentration is proved by experiments to be crucial
and plays an important role in the process of Fur binding/unbinding to DNA,
this constitutes the major part of the sensing process which triggers the
protein binding to DNA. (see metal ion dependence of bond length, Figure 2
Table1) The effect of metal ions radii on binding affinity is clear in the
behavior
Considering the Irving –Williams series: stability of ligand binding follows
the sequence $Mn^{2+}<Fe^{2+}<Co^{2+} \approx Zn^{2+}$, and both cobalt and iron show LFSE
and that of $Co^{2+}> Fe^{2+}$, while both $Mn^{2+}(d^5)$ and $Zn^{2+} (d^{10})$ have no ligand
field stabilization.

Effect of radius on binding

Table2: The standard divalent metal ion radii in high spin octahedral and tetrahedral fields.

Metal ion	Coordination number	Crystal radius	Ionic radius
Fe^{2+}	6 low spin	0.75	0.61
	6 high spin	**0.92**	**0.78**
Mn^{2+}	6 low spin	0.81	0.67
	6 high spin	**0.97**	**0.83**
Co^{2+}	**4 high spin**	**0.97**	**0.83**
	5 high spin	0.81	0.67
	6 low spin	0.79	0.65
	6 high spin	**0.885**	**0.745**
Zn^{2+}	**6 high spin**	**0.88**	**0.74**

The ionic radii of the ions in high spin distorted octahedral environment are of Fe^{2+}, Co^{2+}, Mn^{2+} and Zn^{2+} are shown in Table 2 with the most likely environment shown in bold. Our previous experimental report, [57] Fe Mössbauer spectra and epr spectra of Mn (II) and Cobalt (II) showed that the metal ions are present in a distorted octahedral environment[4][7], while in the case of cobalt (II) a tetrahedral environment cannot be ruled out[7]. Table 1 shows the measured of M^{2+}-Ligand distances for candidate binding residues on the Fur protein, it's evident that upon increasing metal ions' concentration an enhanced binding takes place in both Fur sites as expected from conformational motion in the Fur dimer. All these ions, except Zn^{2+},

have crystal field stabilization energies which contributes to the binding and consequently to DNA binding of Fur upon conformational changes in the dimer. The ability of Fe^{2+}, Co^{2+} and Mn^{2+} to bind the histidine nitrogen and aspartate oxygen plays a role in the co-repressor activity and to produce enough conformational change in the Fur dimer helices to shift the protein closer to DNA Fur box (Figure 1). Fe^{2+} and Co^{2+} ions proved to associate in larger quantities with Fur dimer up to 6:1[7], but maintaining the presence of the two major distorted sites[9][3]. The zinc ion proved to be a weak co-repressor for Fur compared to the other ions , but its binding is enough for Zur to bind DNA[1,10,27,28]
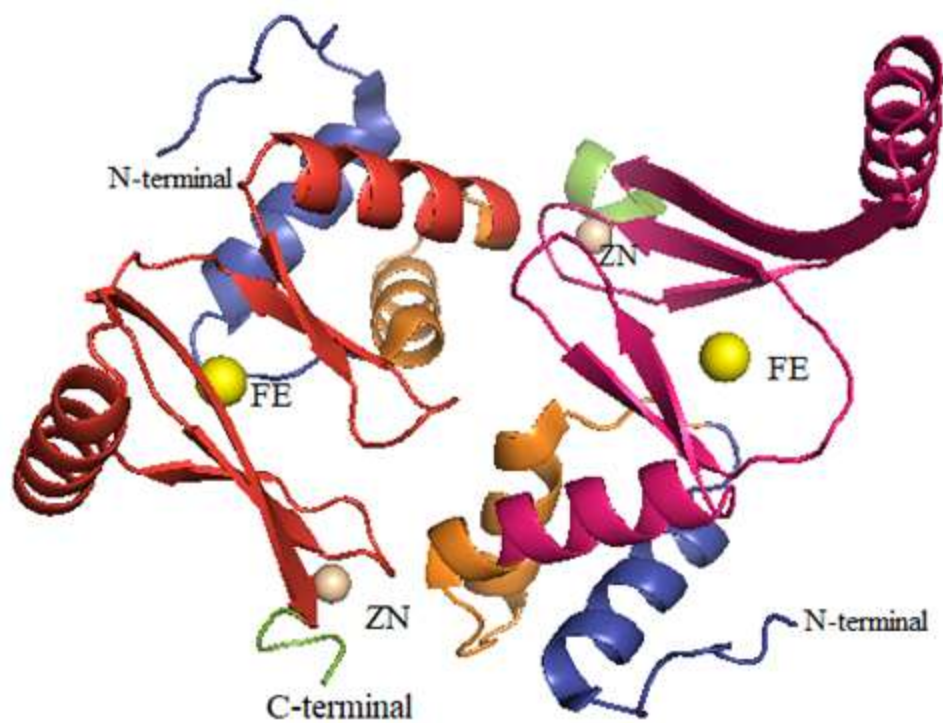
Figure 3: Fur with Zn^{2+} and Fe^{2+}, It shows Zinc ion bound to the zinc site (site 1) near the c-terminal while the Fe atom near the N-terminal. (see Table 1)

The metal ligand distances agree well with our previous experimental work [4], in which Mn (II) bound to one site per Fur monomer with K_d value 85 μM. Fe (II) bound 2 sites on Fur, with stronger binding (K_d 55μM) and when analyzed to site one (K_d 30 μM) and a weaker site (two) (K_d 280 μM). Co(II) showed a strong binding in both tetrahedral and octahedral geometries with K_d 60 μM and a weaker site with K_d 600μM.
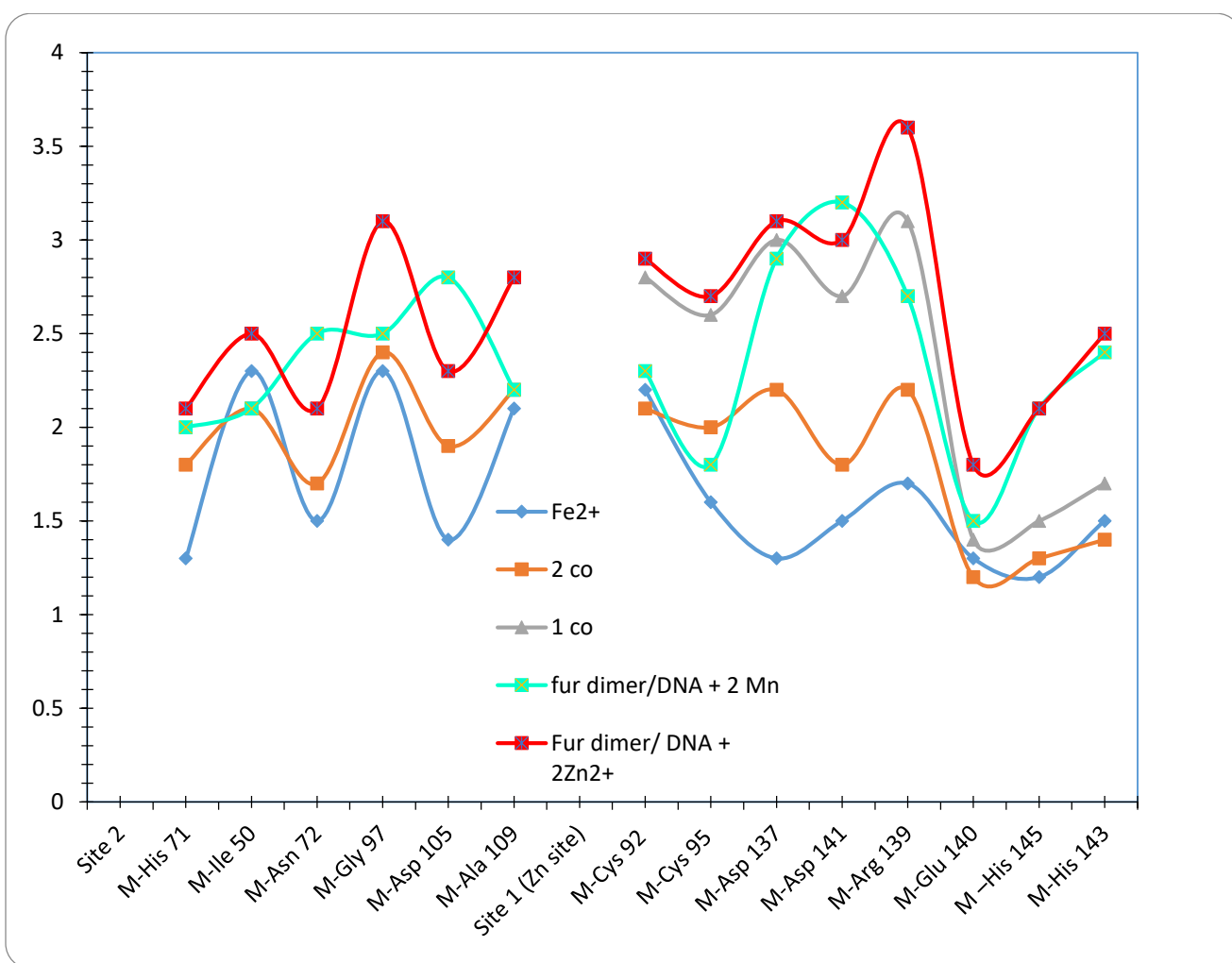
Figure 4 : Data from Table 1 plotted for site one and site two shows that iron and cobalt are tightly bound to residues and it shows that adding a second ion enhances the binding of the first ion
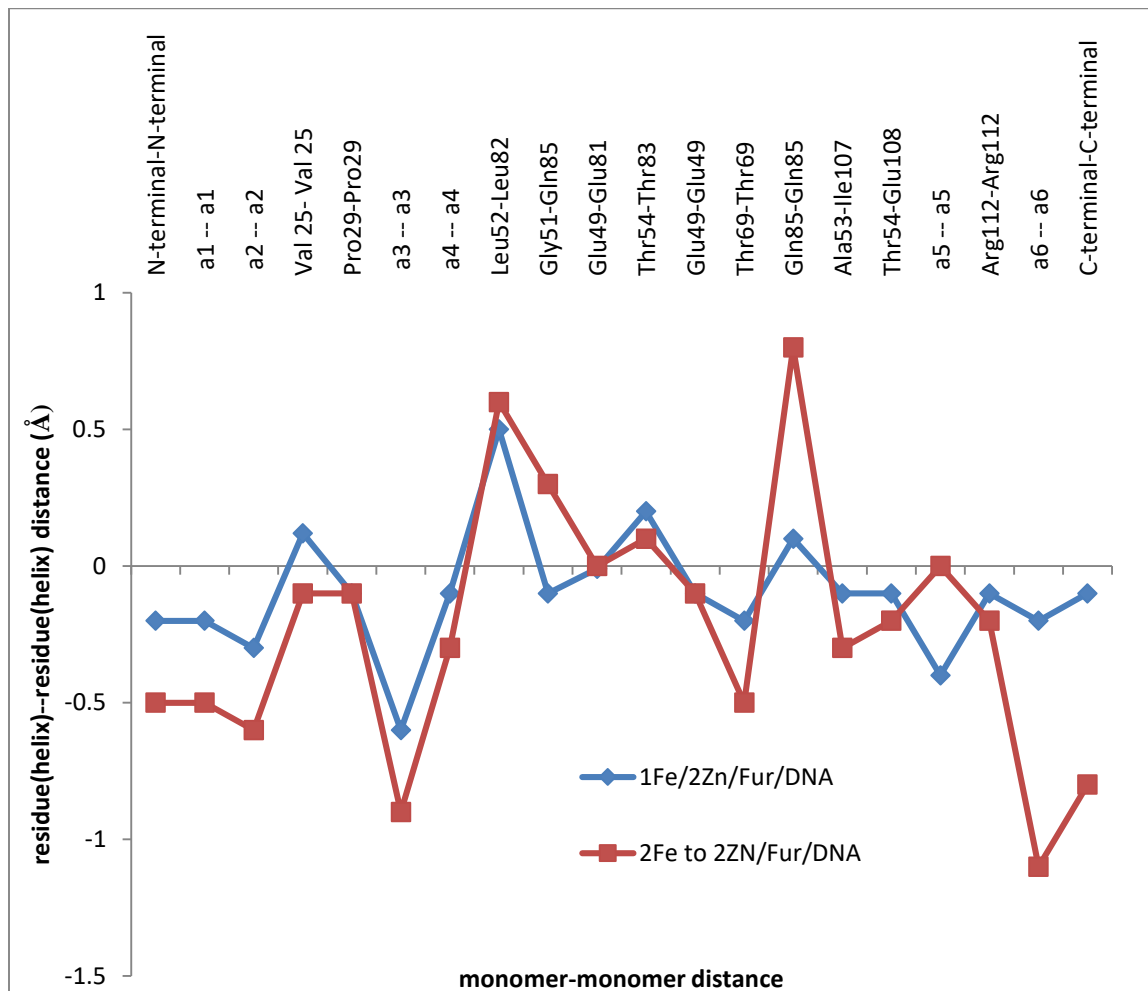
Figure 5 (a): Shifts in Fur-Fur distances in the dimer upon adding metal ions, this shift is represented by key positions on each monomer. The effect of the presence of Zn^{2+} ions on shifting the amino acid residues and helices on each Fur monomer upon increasing Fe^{2+} ion concentration. See Figure 3
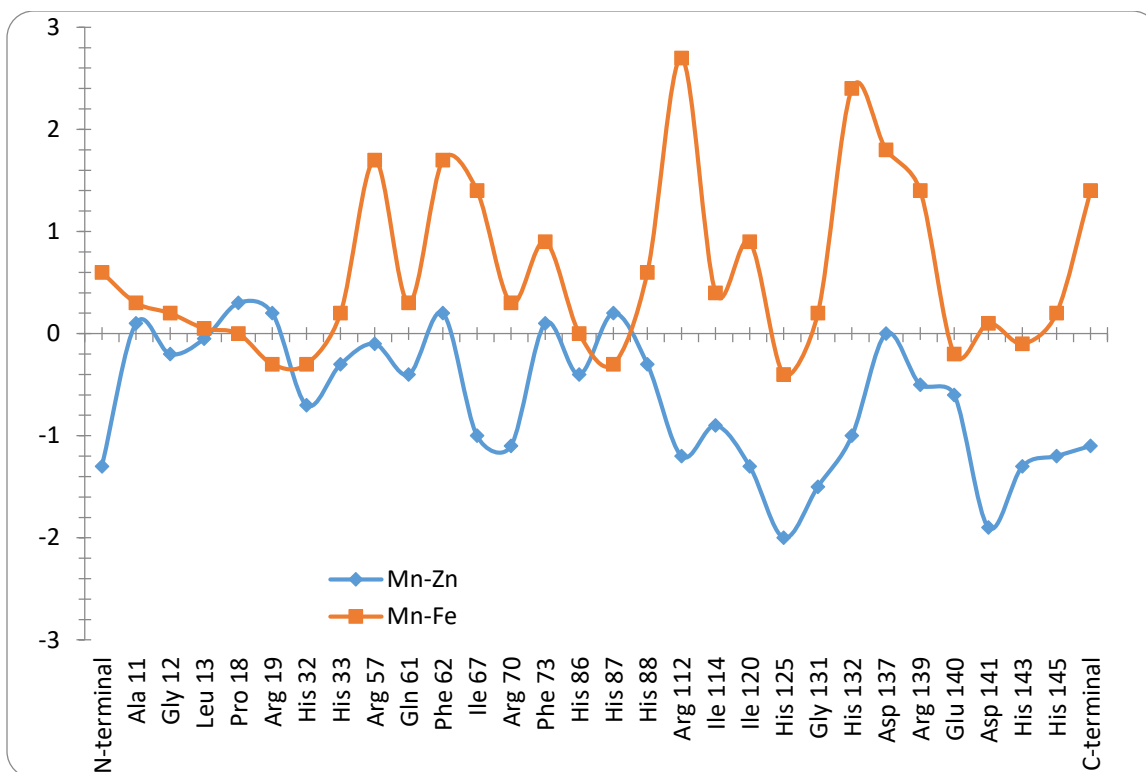
Figure 5 (b): The effect of Mn^{2+} on shifting the amino acid residues closer to DNA was compared with both Fe^{2+} and Zn^{2+}. Mn(II) compared to Zn(II) Blue. Mn(II) compared to Fe(II) orange

Orange positive line in Figure 5 (b) shows that Fe (II) shifts residues about 3Å closer to DNA more than Mn while Blue shows that Mn shifts residues to a maximum of 2A (in case of some residues) closer to DNA more than Zinc, Baring in mind that zinc does not activate Fur to bind DNA makes His 132 and His 125 key residues in the process

The plot (Figures 5) shows that, in general, the shifts towards DNA caused by Mn^{2+} are larger than those caused by Zn^{2+} ion while when compared to Fe^{2+} shifts are less by 1-3 Å or are equal in case of key residues His 143, Asp 141, Glu140, His125, His 87, His 86, His32 and Arg 19 in helices α1, α2, α3[3]

All these residues and helices were affected to the same extent by both Mn^{2+} and Fe^{2+} (same Role in both metal ions in both Mur and Fur proteins, considering the fact that they differ in the affinty of Fur towards each metal ion) Shift around zero, Asp 141, His86 Pro18, Leu13

His143 His125 Glu140, His 87 His32, Arg19 in case of the N-donor ligan residues the shift closer to DNA is slightly more in case of Mn^{2+} due their preference for Mn^{2+}.

Mn^{2+} and Zn^{2+} Both ions bind the Fur dimer (Figure 3), no difference in shifts or slightly more shift for Zn (maximum difference is -2 Å for His125 and Asp141) than in Mn are: for Asp137 (0), Arg57(0) Phe73,Hi86 Hi87 Hi88 Pro18 and Arg19, Phe62, Leu13(0), Ala11(0), the residues which experience a highly negative shifts in Mn compared to Zn , i.e they play crucial role in the case of Mn are: His145,143 Asp141Glu140 His132,Gly131,His125Ile 120,114, 67Arg112,70, His32
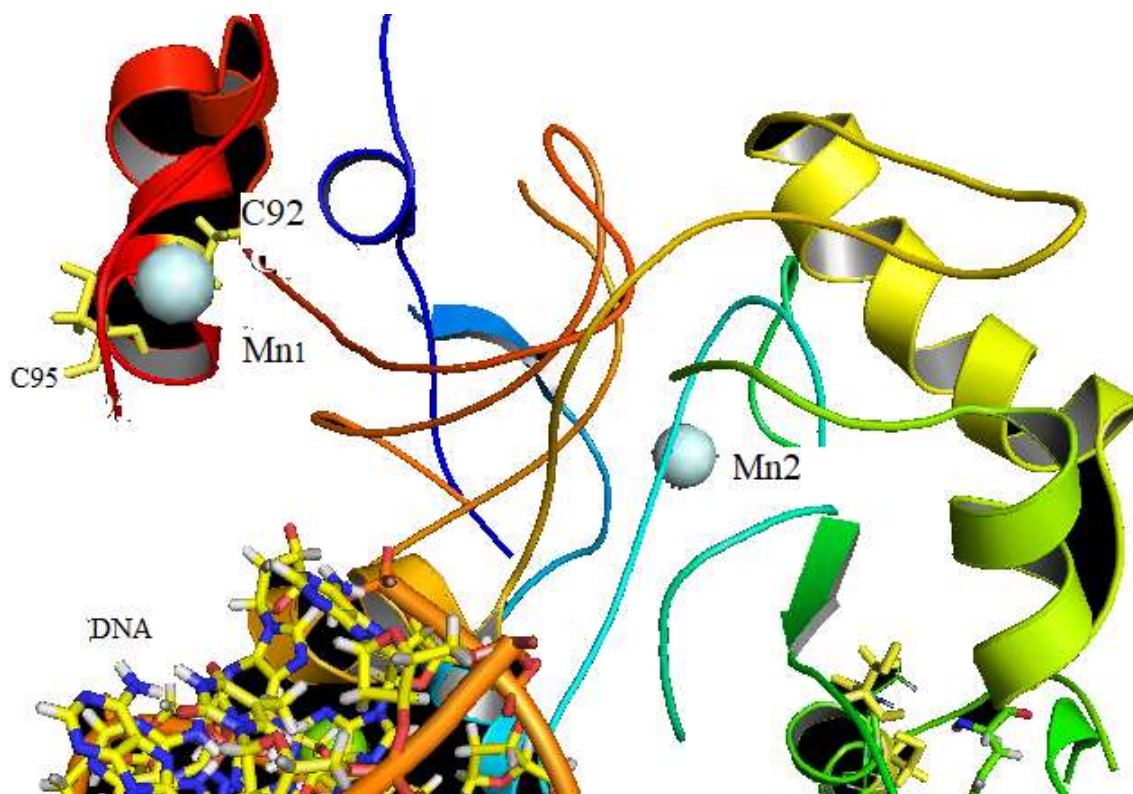
Figure 6: The Binding of Mn(II) to site one(known as Zinc site) and site two near the N-terminal. See Table 1 for detailed binding.

The shifts in amino acid residues with Mn^{2+} was negative compared to the shifts caused by Zn^{2+}(aa residues moved towards DNA to a greater extent than when Zn^{2+} ion is present) , with the exception of Asp137, His87, Phe 73, Phe 62, Arg19, Pro18 and Ala11. Most negative shifts, i.e closest to DNA were observed for Asp141, His125,Arg112. The shifts in amino acid residues closer to DNA caused by Mn^{2+} relative to those caused by Fe^{2+} are positive, i.e the shifts caused by Mn^{2+} are less than those produced by Fe^{2+} with the exceptions of His143 His86 Pro18 Leu13 Asp141 (zero shifts) , Glu140, His125, His87, , His32, Arg19 all slightly negative compared to Fe^{2+}Shifts. This means that His143, His 86, Pro18 Leu13 and Asp141 are affected by Mn^{2+} to a comprable degree as Fe2+ (or Both Fe2+ and Mn2+ have a similar effect on these aa residues). While the shift of Glu140, His 125, His 87, His 32 and Arg 19 induced by Mn^{2+} is stronger than that induced by Fe^{2+}.

Mn^{2+} could activate Fur dimer to bind DNA both in vivo and in vitro with a dissociation constant (85 μM [4],Both Fe^{2+} and Mn^{2+} bind Fur dimer in a 2:1 ratio, i.e. 2 metal centers per Fur dimer[4] Figure 6. Mn^{2+} shifted the residues closer to DNA in a similar manner to Fe^{2+} (K_d 55 μM) with few exceptions. The shifts in residue positions are greater than in the case of Zn^{2+} which is known for its structural role and low activation of Fur [2]. The above amino acid residues are the key residues for Fur activity in its DNA binding. Residues which have preference for Mn (II) binding over Fe (II) are His 143, Asp 141, His 125, His 32 while residues like His 145 and Glu 140 have more preference for Fe(II).

His132 shift closer to DNA in the order Fe>Mn>Zn

His 87 less than Zn^{2+} and both Mn^{2+} an Zn^{2+} more than in Fe^{2+}

Ala11 shifted away from DNA in the order Mn> Zn> Fe

The general trend in conformational change is similar in all three metal ions with minor differences

$\alpha1-\alpha1$, $\alpha2-\alpha2$, Val25-Val25, $\alpha4-\alpha4$, Thr 69-Thr69, Glu85-Glu85 and $\alpha6-\alpha6$ moved closer together in Mn more than both Fe and Zn indicating the strongest conformational change caused by Mn while Gly 51-Gln85 separation increased most for Mn. It seems that when the dimerization region ($\alpha3-\alpha3$, Gly51-Gln85 , Leu52-Leu82 and Glu49-Glu81) moves apart the helices and residues on both N and C terminals move closer together in a reversed motion. The Fur subunits move apart triggering a reversed motion on the other helices and residues to close on DNA

The order of motion is $\alpha6-\alpha6$ >Glu85-Glu85 > $\alpha5-\alpha5$>>$\alpha1-\alpha1$>$\alpha4-\alpha4$

The metal ion sensing part of the protein is probably what is called the structural Zn site[ref] consisting of $\beta3$ which contains Cys92 and 95, and the end coil T11 near the C-terminal[1] . The iron control site consists mainly of parts of the coil (T8) and coil T7 and a contribution from T6

 This will help to figure out the detailed mechanism of the metal ion binding, conformational change and shifting of residues closer to DNA, i.e. how does the Fur senses the metal ion, binds it, and how does the metal ion induce or tune the Fur dimer in order to lock onto the DNA. Since all metal ions including Zn goes first to the cavity or site that is the Zn site or structural site and Fe could easily replace Zn in this site it can be said that metal ions are sensed by residues in this site (Cy 92, Cys 95, His143, His 145, Asp 137, Asp 141, Arg 139 and Glu 140)

References

[1]   N. Baichoo, J.D. Helmann, Recognition of DNA by Fur: A reinterpretation of the Fur box consensus sequence, J. Bacteriol. 184 (2002) 5826–5832. https://doi.org/10.1128/JB.184.21.5826-5832.2002.

[2]   A. Bagg, J.B. Neilands, Ferric uptake regulation protein acts as a repressor, employing iron (II) as a cofactor to bind the operator of an iron transport operon in Escherichia coli., Biochemistry. 26 (1987) 5471–5477.

[3]   M.Y.M.Y. Hamed, S. Al-jabour, Iron(II) triggered conformational changes in Escherichia coli fur upon DNA binding: a study using molecular modeling, J. Mol. Graph. Model. 25 (2006) 234–246. https://doi.org/10.1016/j.jmgm.2005.12.010.

[4]   M.Y.M.Y. Hamed, J.B.B. Neilands, V. Huynh, Binding of the ferric uptake regulation repressor protein (Fur) to Mn(II), Fe(II), Co(II), and Cu(II) ions as co-repressors: Electronic absorption, equilibrium, and 57Fe Mössbauer studies, J. Inorg. Biochem. 50 (1993) 193–210. https://doi.org/10.1016/0162-0134(93)80025-5.

[5]   S. Jabour, M.Y. Hamed, Binding of the Zn2+ ion to ferric uptake regulation protein from E. coli and the competition with Fe2+ binding: A molecular modeling study of the effect on DNA binding and conformational changes of Fur, J. Comput. Aided. Mol. Des. 23 (2009). https://doi.org/10.1007/s10822-008-9251-2.

[6]   M.Y. Hamed, J.B. Neilands, An electron spin resonance study of the Mn(II) and Cu(II) complexes of the Fur repressor protein, J. Inorg. Biochem. 53 (1994). https://doi.org/10.1016/0162-0134(94)85111-5.

[7]   M.Y. Hamed, The Role of Divalent metal ions as co-repressors for the repressor protein FUR: A study of the Co(II) complexes, Fifth International conference on Bioinorganic Chemistry, J.Inorg.Biochem,

43(3),512 (1991). 43 (1991) 512.

[8]　V. De Lorenzo, S. Wee, M. Herrero, J.B. Neilands, Operator sequences of the aerobactin operon of plasmid colV--K30 binding the ferric uptake regulation (fur) repressor, J. Bacteriol. 169 (1987) 2624–2630.

[9]　S. Jabour, M.Y.M.Y. Hamed, Binding of the Zn^{2+} ion to ferric uptake regulation protein from E. coli and the competition with Fe^{2+} binding: A molecular modeling study of the effect on DNA binding and conformational changes of Fur, J. Comput. Aided. Mol. Des. 23 (2009) 199–208. https://doi.org/10.1007/s10822-008-9251-2.

[10]　C. Dian, S. Vitale, G.A. Leonard, C. Bahlawane, C. Fauquant, D. Leduc, C. Muller, H. De Reuse, I. Michaud-Soret, L. Terradot, The structure of the Helicobacter pylori ferric uptake regulator Fur reveals three functional metal binding sites, Mol. Microbiol. 79 (2011) 1260–1275. https://doi.org/10.1111/j.1365-2958.2010.07517.x.

[11]　E.W. Althaus, C.E. Outten, K.E. Olson, H. Cao, T. V. O'Halloran, The ferric uptake regulation (Fur) repressor is a zinc metalloprotein, Biochemistry. 38 (1999) 6559–6569. https://doi.org/10.1021/bi982788s.

[12]　E.E. Zheleznova, J.H. Crosa, R.G. Brennan, Characterization of the DNA-and metal-binding properties of Vibrio anguillarum Fur reveals conservation of a structural Zn^{2+} ion, J. Bacteriol. 182 (2000) 6264–6267.

[13]　D. Bellini, A. Lebedev, R. Keegan, J. Todd, A.M. Hemmings, A.W. Johnston, M.A. Walsh, Structure of a zinc-bound manganese uptake regulator, Mur, To Be Publ. (n.d.) 2210. https://doi.org/10.2210/PDB5FD6/PDB.

[14] S.T. Nader, S., Perard, J., Carpentier, P., Michaud-Soret, I., Crouzy, Ferric uptake regulator with Mn and Zn form Pseudomonas aeruginosa, (n.d.) 2210. https://doi.org/10.2210/pdb6H1C/pdb.

[15] E. Pohl, J.C. Haller, A. Mijovilovich, W. Meyer-Klaucke, E. Garman, M.L. Vasil, Architecture of a protein central to iron homeostasis: crystal structure and spectroscopic analysis of the ferric uptake regulator, Mol. Microbiol. 47 (2003) 903–915. https://doi.org/10.1046/j.1365-2958.2003.03337.x.

[16] S. Wee, J.B. Neilands, M.L. Bittner, B.C. Hemming, B.L. Haymore, R. Seetharam, Expression, isolation and properties of Fur (ferric uptake regulation) protein ofEscherichia coli K 12, Biometals. 1 (1988) 62–68.

[17] M. Coy, The interaction of the ferric uptake regulation protein with DNA, Biochem. Biophys. Res. Commun. 212 (1995) 784–792.

[18] M.Y.Y. Hamed, J.B.B. Neilands, An electron spin resonance study of the Mn(II) and Cu(II) complexes of the Fur repressor protein, J. Inorg. Biochem. 53 (1994) 235–248. https://doi.org/10.1016/0162-0134(94)85111-5.

[19] J. Pérard, S. Nader, M. Levert, L. Arnaud, P. Carpentier, C. Siebert, F. Blanquet, C. Cavazza, P. Renesto, D. Schneider, M. Maurin, J. Coves, S. Crouzy, I. Michaud-Soret, Structural and functional studies of the metalloregulator Fur identify a promoter-binding mechanism and its role in Francisella tularensis virulence, Commun. Biol. 1 (2018). https://doi.org/10.1038/s42003-018-0095-6.

[20] D.A. Case, I.Y. Ben-Shalom, S.R. Brozell, D.S. Cerutti, T.E. Cheatham III, V.W.D. Cruzeiro, T.A. Darden, R.E. Duke, D. Ghoreishi, M.K. Gilson, others, AMBER 2018; 2018, Univ. California,

San Fr. (n.d.).

[21] W.L. DeLano, The PyMOL Molecular Graphics System, (2002).
      http://www.pymol.org.

[22] A. Nurisso, A. Daina, R.C. Walker, Homology Modeling, 2012.
      https://doi.org/10.1007/978-1-61779-588-6.

[23] L.A. Kelley, R.M. MacCallum, M.J.E. Sternberg, Enhanced genome
      annotation using structural profiles in the program 3D-PSSM, J. Mol.
      Biol. 299 (2000) 501–522. https://doi.org/10.1006/jmbi.2000.3741.

[24] M.A. Sheikh, G.L. Taylor, Crystal structure of the Vibrio cholerae
      ferric uptake regulator (Fur) reveals insights into metal co-ordination,
      Mol. Microbiol. 72 (2009) 1208–1220. https://doi.org/10.1111/j.1365-
      2958.2009.06718.x.

[25] S.S. Narang, D. Goyal, B. Goyal, Inhibition of Alzheimer's amyloid-
      β42 peptide aggregation by a bi-functional bis-tryptoline triazole: key
      insights from molecular dynamics simulations, J. Biomol. Struct. Dyn.
      38 (2020) 1598–1611.
      https://doi.org/10.1080/07391102.2019.1614093.

[26] M. Coy, J.B. Neilands, Structural dynamics and functional domains of
      the Fur protein, Biochemistry. 30 (1991) 8201–8210.

[27] S.A. Mills, M.A. Marletta, Metal binding characteristics and role of
      iron oxidation in the ferric uptake regulator from Escherichia coli,
      Biochemistry. 44 (2005) 13553–13559.
      https://doi.org/10.1021/bi0507579.

[28] E. Bai, F.I. Rosell, B. Lige, M.R. Mauk, B. Lelj-Garolla, G.R. Moore,
      a G. Mauk, Functional characterization of the dimerization domain of
      the ferric uptake regulator (Fur) of Pseudomonas aeruginosa.,
      Biochem. J. 400 (2006) 385–92. https://doi.org/10.1042/BJ20061168.